Spinnability and Physical Properties of *In Situ* Composite Fibers Based on Thermotropic Liquid Crystalline Polymer

Xiaojun He, Michael S. Ellison, Rajesh P. Paradkar

School of Materials Science & Engineering and The Center for Advanced Engineering Fibers and Films, 161 Sirrine Hall, Clemson University, Clemson, South Carolina 29634-0971

Received 29 May 2001; accepted 16 October 2001

ABSTRACT: *In situ* composite fibers based on poly(ethylene 2,6-naphthalate) (PEN) and a thermotropic liquid crystalline polymer (Vectra A950) were prepared using a single-screw extruder. The fibers were taken up at selected speeds. The spinnability, thermal behavior, mechanical properties, and morphologies of the PEN/Vectra A950 blend were investigated. The results showed that the PEN/Vectra A950 blends were partly miscible, and the miscibility increased with the increased concentration of Vectra in the blend. The DSC measurements indicated that Vectra enhanced the crystallization process of PEN by performing as a nucleating agent. The Instron tensile property study, coupled with scanning electron microscopy, revealed that the mechanical properties of the PEN matrix were significantly improved when Vectra existed as long and continuous fibrils. The laser Raman results showed that the Vectra orientation began to develop at take-up speeds above 500 m/min. © 2002 Wiley Periodicals, Inc. J Appl Polym Sci 86: 795–811, 2002

Key words: blends; fibers; liquid crystalline polymers; morphology; Raman spectroscopy

INTRODUCTION

Poly(ethylene naphthalate) (PEN), a polyester produced via a polycondensation reaction, was commercialized by Eastman Chemical Company in 1994 as a so-called high performance polymer for engineering applications. Current attention is focused on potential applications of PEN in fibers, especially because of its better properties compared to other polyesters. The large and stiff naphthalene double ring in PEN makes it more linear than poly(ethylene terephthalate) (PET), which confers a higher glass-transition temperature (T_g), improved thermal stability, and higher melt viscosity on PEN as compared to PET. Accordingly, although PEN chips therefore do require higher extrusion temperatures, PEN can be processed on equipment designed for PET.

Thermotropic liquid crystalline polymers (TLCPs) have also attracted considerable attention in recent years. They are the preferred reinforcing materials for designing *in situ* composites, because of their ability to be processed into highly oriented fibrils when mixed with other thermoplastic polymers. The resulting *in situ* composite system, compared to the chopped glass filled system, facilitates processing, such as lower processing energy requirements and lower melt viscosity, and has good recyclability. There were numerous studies on *in situ* composites based on TLCPs and commercial thermoplastic polymers. Many of those can be found in the review by Dutta et al.[1] Reports on fiber formation from TLCP/thermoplastic polymer blends are scarce, which is probably due to the narrow processing window of these two kinds of polymers. Because of their rigid backbone structure, TLCPs usually require high processing temperatures while most thermoplastic polymers degrade at those temperatures. Difficulties regarding the spinning of TLCP/thermoplastic polymer blends were reported by La Mantia et al.[2]

The objectives of this article are to present the results of our investigation into the spinnability of PEN blended with various amounts of TLCP using a single-screw extruder and to report on our analysis of the relationship among the processing parameters, morphology, and mechanical properties of PEN/TLCP composite fibers.

EXPERIMENTAL

Polymers

The TLCP used in this work is Vectra A950 produced by the Ticona Company. It is a random liquid crystalline copolyester containing 73 mol % 4-hydroxybenzoic acid (HBA) and 27 mol % 6-hydroxy-2-naphthoic acid, with a T_g of 113°C, a melting temperature (T_m) of 282°C, and a specific gravity of 1.4 g/cm^3 as reported by Ticona. The PEN was obtained from Eastman Com-

Correspondence to: M. S. Ellison (ellisom@clemson.edu).

Contract grant sponsor: National Science Foundation; contract grant number: EEC 9731680.

TABLE I
Take-Up Speeds Employed for Composition Values of PEN/TLCP Blended Fibers

TLCP content (%)	Take-up speed (m/min)
5	300
10	300
20	300
30	250
	300
	400
	500
40	300
50	300
50	300
	400
	500
	600
	700
	800
75	300
100	300

pany (Kingsport, TN). The reported T_g and T_m of this PEN are 120 and 267°C, respectively, and the specific gravity is 1.34 g/cm^3.

Rheology

Rheological measurements were carried out using an Instron model 3210 capillary rheometer. Before the measurement, the PEN and Vectra polymer chips were dried for 24 h at 120°C in a vacuum oven. A die with a length to diameter ratio (L/D) of 40 was used. The measurements were carried out at 310, 315, and 320°C. The barrel friction test, which was run by letting the plunger go through the empty barrel after each measurement, was used to correct the force exerted on the polymer melt. The common correction for the shear rate was also made.

Melt spinning

The PEN and Vectra A950 chips were mixed by manual stirring and then dried in a vacuum oven at 120°C for 24 h prior to melt spinning. The weight percentages of Vectra A950 used in the study were 0, 5, 10, 20, 30, 40, 50, 60, 75, and 100. The melt blends were extruded using a Hills, Inc., 1-in. single-screw extruder with a L/D ratio of 30:1 in the Fiber & Polymer Science research facilities of the School of Materials Science & Engineering at Clemson University. A three-hole spinneret with a hole diameter of 1 mm and a L/D ratio of 4 was used to obtain the fibers. A four-zone temperature profile (290, 306, 306, and 306°C) on the extruder was used for spinning the PEN/Vectra A950 blends. Fibers were collected at selected take-up speeds (TUSs) to effect changes in the spin line tension (Table I).

Differential scanning calorimetry (DSC)

The thermal properties of all the fibers and the starting materials were investigated using a TA Instruments DSC 2920 calorimeter in a nitrogen atmosphere. Samples with masses of 3–5 mg were initially heated from 25 to 310°C at a heating rate of 5°C/min, and then they were held isothermal at that temperature for 5 min. This was followed by cooling to room temperature at a rate of 10°C/min. Three runs were performed for each data point.

Thermogravimetric analysis (TGA)

The thermal stability of PEN and Vectra during the residence time in the extruder was determined via TGA. The TGA system we used was a TA Instruments TGA 2950 analyzer. The PEN and Vectra A950 samples were initially immediately heated to 330°C and then held isothermal at that temperature for 1 h under an air flow.

Mechanical properties testing

The mechanical properties of all fibers were measured using an Instron model 5582 tensile testing machine. Prior to testing, the diameter of the monofilament was determined with an optical polarizing microscope (MP 3500 series) at an original magnification of 100. The denier (g/9 km) of the fiber was calculated according to the following equation:

$$\text{denier} = (\text{dia})^2 \times 9 \times \pi \times 10^5 \times \rho/4 \qquad (1)$$

where dia is the diameter of the fiber (cm) and ρ is the specific gravity (g/cm^3), which can be calculated for the blends by a simple addition law. (The data in Table II are normalized to the mass of PEN. When considered on the basis of the absolute value of enthalpy, the rule of mixing does apply.) Each fiber was tested at a gauge length of 10 mm and a cross-head speed at 10 mm/min. All the reported mechanical data were the average of at least eight independent measurements.

Scanning electron microscopy (SEM)

The microstructures were characterized by SEM on a Hitachi 3500N microscope at 15 kV and with an aperture size of 3. The samples were collected by rapidly quenching the extrudate in ice water as it exited the spinneret. The extrudates were then freeze-fractured in liquid nitrogen and gold sputtered in preparation for the microscopy. The morphologies of the TLCP in the drawn fibers were also determined by SEM of the fracture surface from the fiber tensile tests. The fractured surface was coated with gold and observed by SEM as above.

TABLE II
Thermal Properties of PEN/Vectra A950 Blends

PEN composition TLCP	T_g (°C)	T_{cc} (°C)	Crystallization enthalpy[a] (J/g)	T_m for PEN/Vectra (°C)	Melting enthalpy[a] (J/g)
100/0	116.2	169.3	34.95	264.88/Undetectable	45.54
95/5	116	158.5	27.87	265.3/Undetectable	43.66
90/10	116.7	156.84	25.48	264.6/Undetectable	42.68
80/20	116.9	153.31	21.62	264.15/Undetectable	43.52
70/30	116.04	151.66	19.48	264.10/Undetectable	45.55
60/40	117.2	151.02	20.24	264.04/Undetectable	47.53
50/50	117.2	149.67	20.61	263.9/Undetectable	52.44
40/60	118.7	150.4	25.76	263.3/Undetectable	57.3
25/75	ND	139.25	18.99	260/282	46.12

ND, not detected.
[a] The enthalpy is normalized to the mass of PEN.

Laser raman spectroscopy

The Raman spectra were collected using a Renishaw System 1000 Raman spectrometer coupled to a Leica DMLM microscope. The other components of the system included a 26-mW 785-nm diode laser, a stigmatic single spectrograph, a two-dimensional thermoelectrically cooled CCD camera, and a personal computer. Raman spectra were obtained from a single fiber specimen using a 50× objective. The spectral range covered 400–1800 cm^{-1} with an approximate spectra resolution of 5 cm^{-1}. The typical data acquisition time was 55 s. We utilized Raman spectroscopy in other studies of fiber microstructure.[3] All data acquisition was performed using the Renishaw WiRE v1.3.15 software. Data were subsequently transferred into GRAMS/32 (Galactic Inc., Salem, NH) for processing and analysis. The raw Raman data were smoothed (binomial), followed by subtracting a linear baseline from each spectrum. The areas under the peak of interest (1599 cm^{-1}) were then estimated using the standard curve-fit routine in GRAMS/32. The peak was fitted multiple times to ensure the reproducibility of the fit. A mixed Gaussian–Lorentzian function was used throughout, although the peaks were found to be predominantly Lorentzian. The area enclosed by the 1599 cm^{-1} band, which was calculated in the same manner in subsequent calculations of orientation, was used as the reference intensity value. This is discussed further in the Results and Discussion section.

Polarized Raman spectra are denoted using the standard "Porto" notation.[4] For backscattering geometry as used in the Raman microscope and the Z axis as the macroscopic fiber axis (i.e., draw direction) we can write $Y(ab)Y'$, where Y and Y' denote the directions of propagation of the incident and scattered light, respectively, and a and b denote the direction of the polarization of the electric vector of the incident (a) and scattered (b) laser radiation. Thus, $Y(ZZ)Y'$ (abbreviated as the ZZ spectrum throughout this article) denotes the Raman spectrum of PEN/TLCP fibers obtained when the incident laser polarization was set parallel to the draw direction of the fiber and the scattered radiation was polarized parallel to the incident laser radiation (i.e., the draw direction that was analyzed). By the same token, $Y(XX)Y'$ (abbreviated here as XX) indicates that the incident laser polarization and the analyzed Raman scattering are both polarized perpendicularly (radial) to the fiber draw direction.

RESULTS AND DISCUSSION

Effects of processing parameters on fibril formation of TLCPs in matrix polymer

As we mentioned earlier, when blended with thermoplastic materials the TLCP molecules have a tendency to align and orient to form fibrillar structures under appropriate processing conditions, thereby imparting enhanced mechanical properties to the thermoplastic polymer blends. Many studies were conducted to explore various possibilities for control of TLCP fibril formation in the matrix polymer. Generally speaking, fibril formation is determined by the flow conditions, the viscosity ratio of the TLCP to the matrix polymer, the Weber number (the ratio of the viscous stress to the interfacial stress between the two phases), the mixture composition, and the initial size of the TLCP droplets. Among these factors, the most important is the viscosity ratio of TLCP to the matrix polymer.

Imposed stresses cause dispersed domains to deform and break into smaller ones, and coalescence is a competing process. The generation of a new interfacial area requires the expenditure of mechanical energy with increased energy requirements in highly viscous fluids. It was proved[5] that when the viscosity and elasticity of the minor component are greater than that of the major component, the minor component will be coarsely dispersed; when these characteristics are reversed, the minor phase will be finely dispersed. Because the viscosity of TLCP is highly temperature

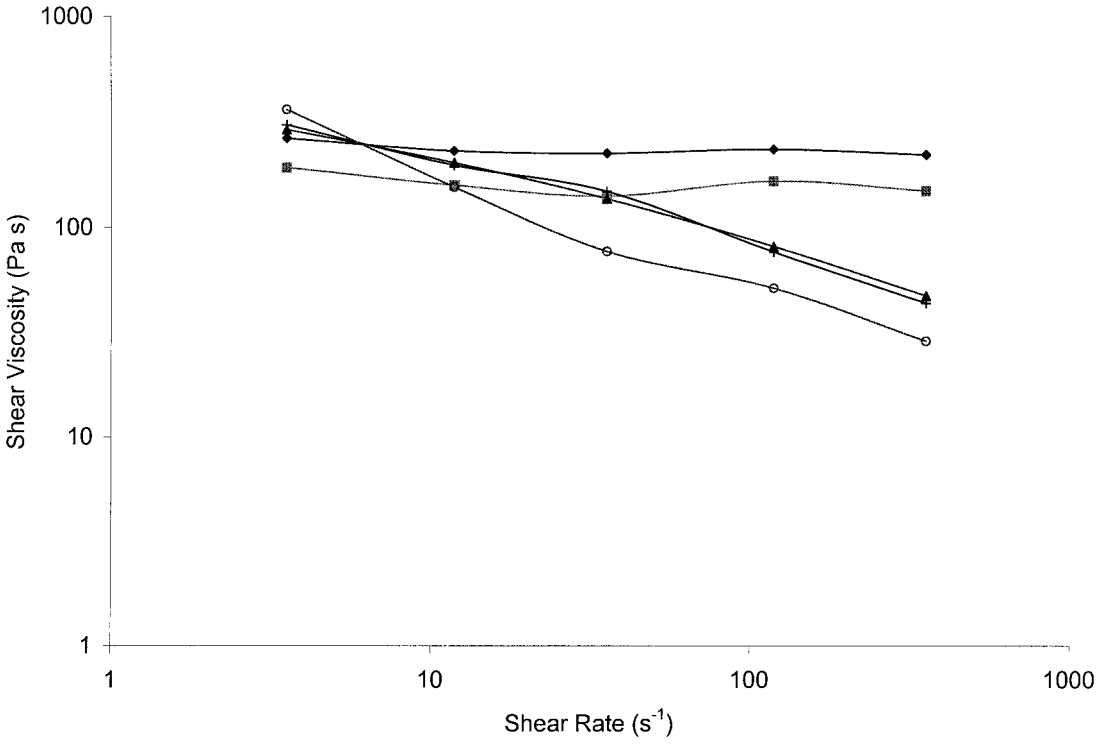

Figure 1 A comparison of the shear viscosity versus the shear rate of PEN and Vectra A950 at 310, 315, and 320°C: (◆) PEN at 310°C, (■) PEN at 315°C, (▲) Vectra A950 at 310°C, (+) Vectra A950 at 315°C, and (○) Vectra A950 at 320°C.

dependent, the fibrillation of TLCP must be highly dependent on this parameter.

Baird and Sun[6] established the processing window for a Vectra A950/polyetherimide blend using the temperature dependence of the dynamic mechanical properties of the materials. The upper processing temperature for each polymer was the temperature at which the rheological property of the polymer remained stable over a certain period of time. To determine the lower processing limit, they measured the storage modulus (G') and loss modulus (G'') of the polymer as it was cooling from the melt. The temperature at which G' was equivalent to G'' was defined as the lower processing limit. The overlapped processing temperature range for both polymers was the processing window for the blending system.

The capillary rheological study undertaken in our lab to find the optimum spinning temperature of PEN/Vectra A950 blend provided us with a good understanding of the relationship between the spinning temperature and the flow behavior of the polymers (Fig. 1). The data show that PEN is essentially a Newtonian fluid over the entire shear range employed; in contrast, Vectra A950 deviates from a Newtonian fluid by exhibiting shear thinning. The data also show that at 310°C the viscosity of Vectra A950 is lower than that of PEN, independent of the shear rates. On the other hand, at 315°C Vectra only exhibits a lower viscosity than PEN at the higher shear rate range, suggesting that the spinning temperature should not be higher than 310°C to obtain a finely structured minor phase Vectra. This result is consistent with other literature reports. Sarlin and Tormala[7] reported that the melt strength of Vectra A950 was drastically reduced at temperatures higher than 310°C, and Haile and Caldwell[8] reported that PEN was easily spun at temperatures ranging from 305 to 310°C. Our rheology data and the literature results corroborate that the processing temperature we chose for PEN/TLCP blends is effective in achieving a fibrillar structure for TLCP.

There is an additional reason that the processing temperature is extremely important for polymer blends containing TLCPs. Lin and Winter[9] reported the formation of crystallites with fewer defects after annealing of Vectra A above the solid–nematic transition temperature. There was also a recent report[10] concerning the degradation of Vectra A950 during heating. Carbon dioxide was the dominant product in all the degradation processes; other reactions, such as crosslinking and oxidation, occurred at different stages of degradation. Therefore, the viscosity ratio, which was demonstrated to have a strong influence on droplet deformation, would be significantly affected by degradation. Our TGA results (Fig. 2) did not show any significant weight loss due to degradation for Vectra A950 while the PEN degraded much faster compared to Vectra at extended times. Even so, the observed weight loss was not considered significant

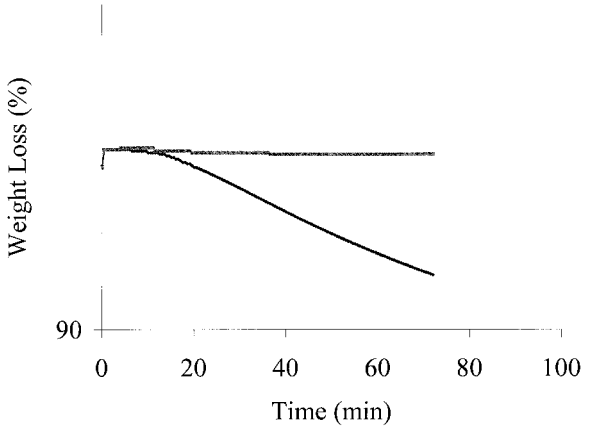

Figure 2 The weight loss versus time for (■) Vectra A950 and (◆) PEN at 330°C.

over the relatively short times corresponding to the residence time in the extruder (Fig. 2).

The TLCP concentration in the blends is the next important factor contributing to the formation of fibrils. There are some inconsistencies in the literature regarding the critical concentration of the TLCP phase for fibril formation. Blizard and Baird[11] studied the development of TLCP morphology in nylon 6,6 and polycarbonate (PC) blended with 60% HBA/PET. They found that at 10 wt % TLCP the TLCP phase was dispersed as droplets. The reason proposed by those authors was that the concentration of TLCP was too low to allow the coalescence of droplets necessary for fibril formation. There were other studies[12] showing that fibrillation did occur at correspondingly low TLCP concentrations. The results of our SEM study of fibrillar morphology development show tacit agreement with those of Blizard and Baird[11] [Fig. 3(a–f)]. It can be clearly seen that TLCP fibrillation begins at 20 wt % TLCP and a TLCP network structure starts to form at a composition of 60 wt %; we conclude that at this composition a phase inversion takes place that changes the TLCP from the minor phase to the major phase.

Other processing parameters such as quench and prespinning drying conditions also play a role in forming TLCP fibrils. Blizard et al.[13] studied the effect of heat transfer on the rheology of TLCP and PC. It was surprising to them to find that TLCP exhibited a sharp increase in viscosity when it was cooled and crystallized. At a particular temperature, the viscosity of TLCP was equal to that of PC; hence, no further deformation of the TLCP phase could happen. In our work we maintained the molten state of Vectra A950 for an extended duration during spinnng by using no quench air and a higher throughput rate.

It was reported that, as the two kinds of polyesters were mixed and passed through the spinneret capillary, an interchain reaction (ester-exchange reaction or transesterification) was introduced. The constitution of the blend is therefore subject to change because of the formation of a block copolymer structure resulting from the transesterification.[14] This reaction may be significantly accelerated by any residual moisture in the polymer.[15] Transesterification could lead to a loss of the mesophase through dilution of the rigid molecular fragments (i.e., TLCP) by the more flexible ones (PEN). To minimize the degree of this reaction during the mixing of two polymers in the extruder, we processed the blends at relatively high extruder speeds to reduce the residence time. The SEM photomicrographs clearly show that the TLCP phase was elongated by passage through the spinneret, implying the success of this strategy in controlling transesterification.

DSC study

Study of the thermal transition behavior of polymer blends may provide important information concerning compatibility, as well as crystallization. The DSC measurements made on our composite fibers over the whole composition range are shown in Figure 4. The fibers comprised mixtures of PEN and Vectra A950 having melting temperatures of 265 and 282°C, respectively. The numerical data are summarized in Table II. Three kinds of transitions are observed in the DSC heating curves: a glass transition (T_g), characteristic of blends, at around 115°C; an exothermic peak, corresponding to the cold crystallization (T_{cc}) of PEN; and an endothermic peak from the melting of PEN (T_m). The T_{cc} of the composite fibers is at least 10°C lower than that of pure PEN, irrespective of composition; the change in T_m is not remarkable or constant. The observed single melting point of PEN shows a minimal decrease from 265 to 263°C up to 60 wt % Vectra. A further increase in the amount of Vectra to 75 wt % results in phase separation of the PEN and Vectra, as evidenced by the occurrence of two melting peaks in the DSC curve. The lower one (260°C) is the melting peak of PEN, and the higher one (282°C) corresponds to the melting peak of Vectra.

Melting temperature depression in a blend is associated with a strong interaction between the two phases. Tang et al.[16] studied the NMR of a PET and Vectra A950 blend. The results from their NMR experiments indicated that PET in the gauche conformation was the preferred conformation at the Vectra–PET interface. Because the free volume of gauche conformers was relatively large, the diffusion of Vectra into the amorphous regions of PET during melting was facilitated. Those Vectra molecules in the amorphous region of PET acted as "impurities" and lowered the melting temperature of PET. We are confident that the same argument is applicable to our PEN/Vectra blend.

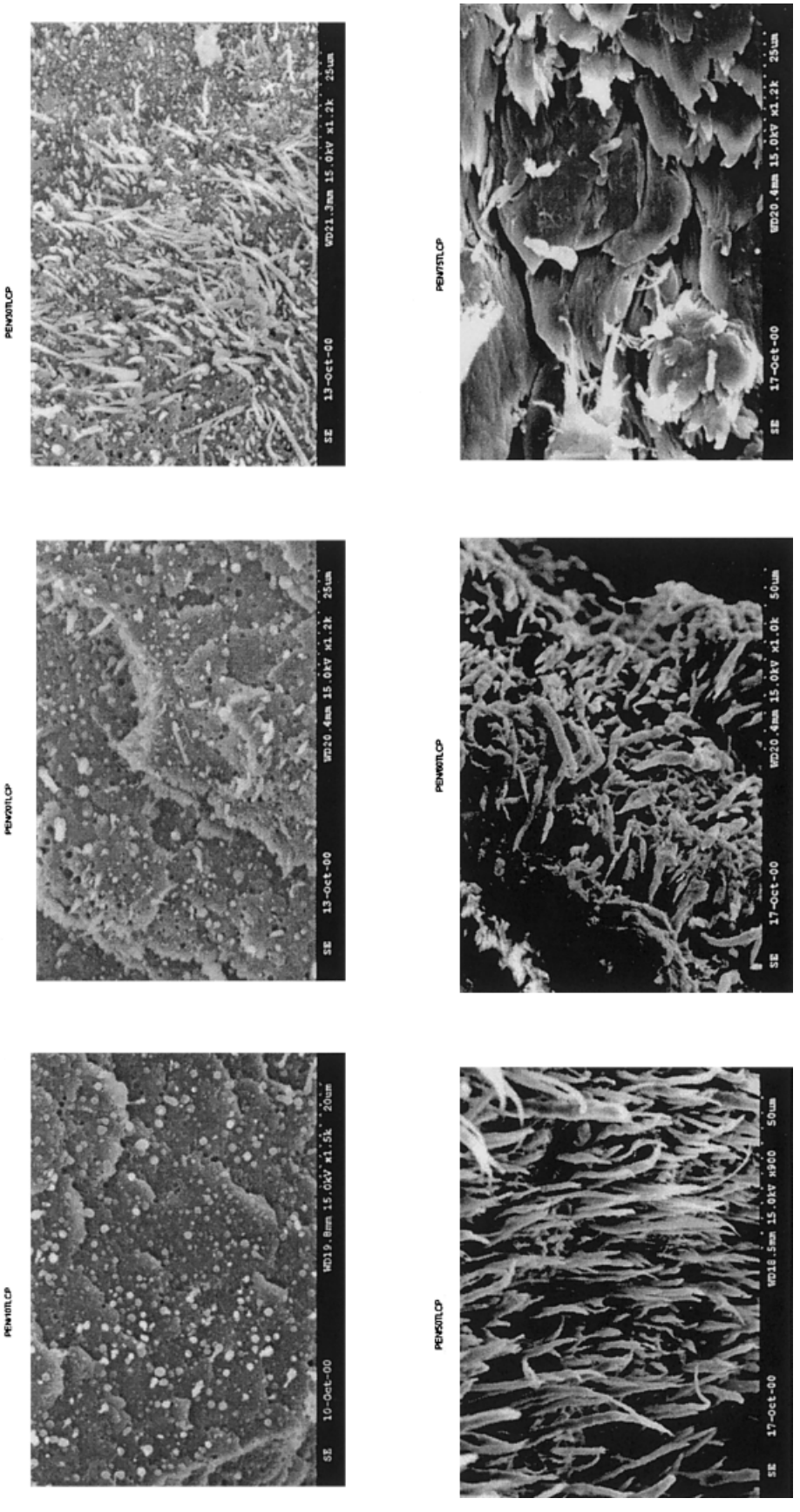

Figure 3 SEM photographs of extrudates containing different concentrations of TLCP.

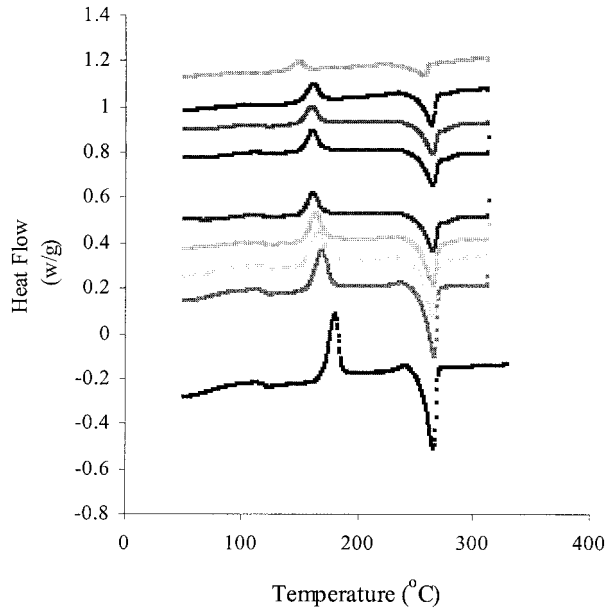

Figure 4 DSC curves for PEN/TLCP blend fibers at a TUS of 300 m/min. The curves from bottom to top are for PEN, PEN/5TLCP, PEN/10TLCP, PEN/20TLCP, PEN/30TLCP, PEN/40TLCP, PEN/50TLCP, PEN/60TLCP, and PEN/75TLCP.

To quantitatively characterize such an interaction between PEN and TLCP, we use the Nishi and Wang[17] equation, while recognizing that it may be more suitable for a two polymer blending system for which thermodynamic interdiffusion exists. The equation was derived from Scott's equation[18] based on an extension of the Flory–Huggins lattice theory. According to that theory, the equation for melting temperature depression is

$$\frac{1}{\phi_1}\left[\frac{1}{T_m}-\frac{1}{T_m^0}\right] = -\frac{BV_2\phi_1}{\Delta H_2 T_m} \tag{2}$$

$$\chi = \frac{BV_1}{RT_m} \tag{3}$$

where T_m and T_m^0 are the melting temperatures of pure PEN and PEN in the blends, respectively; ΔH_2 is the heat of fusion of 100% crystallized PEN (190 J/g from Bucher et al.[19]); V_2 is the molar volume of the polymer repeat unit for PEN; V_1 is the molar volume of the minor phase; and R is the gas constant. The Flory–Huggins parameter χ describes the degree of interaction between the two polymers. A negative value of χ suggests that two polymers are accorded a strong interaction. As a result, a blend based on those two polymers would have good miscibility: the more negative the value, the better the miscibility. Conversely, a positive value of χ indicates that the two polymers exhibit gross phase separation; that is, the two polymers are totally immiscible on the macroscopic scale.

Our data presented as a plot of $1/\phi_1[1/T_m - 1/T_m^0]$ versus ϕ_1/T_m (Fig. 5) shows a linear relationship. The 60% blend deviates from this line or relationship because of phase inversion, which means that TLCP no longer acts as a diluent. Forcing the regression line through the origin, one can obtain the value of B from the slope of the line. From this, the value of χ can be obtained. The χ value determined for the PEN/Vectra blending system is -0.146. The negative sign, together with the small magnitude, indicates limited miscibility exists between the two phases.

Other evidence of interaction between PEN and Vectra is that Vectra facilitates the crystallization of PEN, possibly by functioning as a nucleating agent. One effect of this can be seen in the melting enthalpy of the blend. These heats of fusion (ΔH_m) were normalized to the mass of PEN. The plot first shows an initial drop in the ΔH_m value as TLCP is added to the PEN. This is followed by a continuous increase from 30 wt % TLCP up to 60 wt % TLCP. The enthalpy (ΔH_m) then drops again when the TLCP concentration is 75 wt %. Phase separation begins at this concentration.

It is well known that the crystallization of polymers depends on the probabilities of nucleation and subsequent growth of the nuclei. The growth of nuclei is a transport process, which means the polymer chains or chain fragments self-diffuse onto the existing nuclei and pack themselves into the crystal lattice. Theoretical study shows that the crystallization rate is strongly dependent on the activation energy for the diffusion process at the interface and the free energy of formation of a surface nucleus.[20] A surface nucleus refers to a location on a preexisting crystalline structure, which functions as a nucleation site as opposed to the nucleus that initiates the crystallization. The above heat of fusion data demonstrate that the crystallization process of PEN is facilitated in the high TLCP concentration blend. As we mentioned earlier, the TLCP apparently functions as a nucleating agent during the crystallization of PEN/TLCP blends. The TLCP concentration influences the crystallization of PEN in two

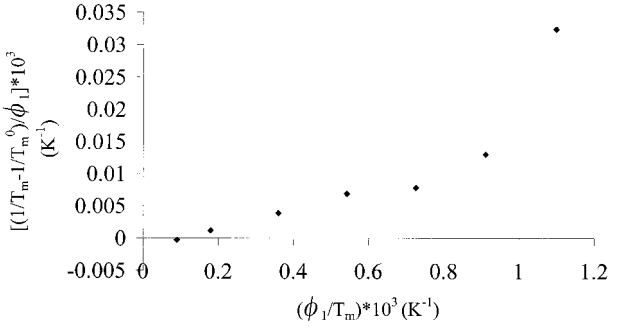

Figure 5 The determination of the Flory–Huggins interaction parameter by using the Nishi–Wang equation.

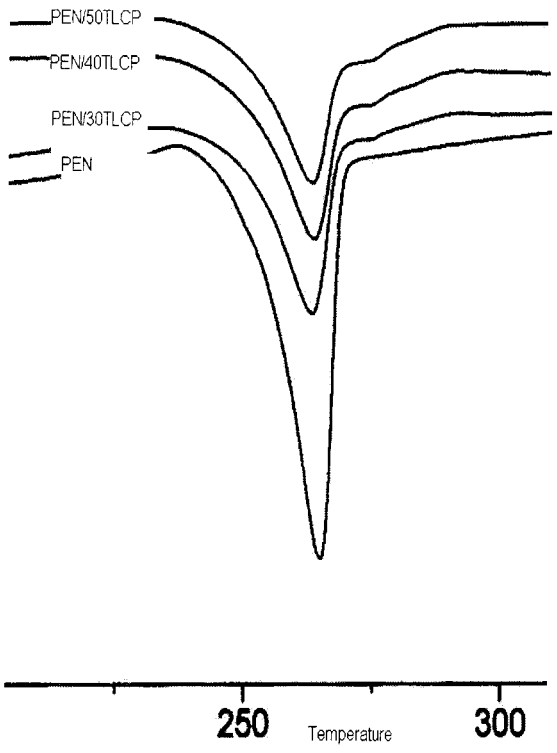

Figure 6 The effect of the TLCP concentration on the shape of the melting peak.

processes. The preceding SEM microphotographs [Fig. 3(a–f)] show that the TLCP phase is more finely dispersed in the blend with a higher concentration of TLCP, which means the interface area per volume is enlarged; therefore, the formation of surface nuclei is accelerated. Meanwhile, because the number of surface nuclei is increased with the increase of the TLCP concentration, the reptation type diffusion of polymer chains onto the surface nuclei becomes easier because of the decrease in the mean free path length of the molecules. It is thus possible for us to conclude that the nucleation efficacy of TLCP is greater for blends with a higher TLCP content.

It is noteworthy that the shape of the melting peak shows a change corresponding to a TLCP concentration over 30 wt % (Fig. 6). Notice that there is a subtle melting peak appearing around 267°C as the TLCP content is over 30 wt %. This peak becomes more obvious as more TLCP is added to the blend, until at 75 wt % TLCP, phase separation takes place and the peak disappears. We believe that the appearance of this subtle peak may be a consequence of the improved miscibility of PEN and TLCP phases occasioned by the increase in TLCP content. During Herlingen et al.'s study[21] on poly(butylene terephthalate) (PBT)/PET blends, they also found a second peak appearing on the DSC curve when the concentration of PBT and PET were equal. They believed that the peak could be attributed to the transesterification reaction at the interface of PET and PBT, which would produce a mixed copolymer. There are several recent reports pointing to a far greater compatibility between polyesters and TLCP that is attributable to the transesterification occurring at the interface.[22,23] Our DSC data show a significant change in the T_m and ΔH_m as the TLCP concentration reaches 30 wt %. It may be concluded that the subtle peak is due to the transesterification between PEN and TLCP at their interface.

Figure 7 describes the relationship between ($\Delta H_m - \Delta H_c$) and the TLCP content. These data were collected at a constant TUS. The ΔH_m is the heat flow when all the crystallites are melted, and ΔH_c is the heat flow associated with crystallization developed during DSC measurement. Hence, the value of ($\Delta H_m - \Delta H_c$) gives some indirect information on the crystallinity before DSC measurement: we believe this crystallinity is that developed during spinning. The increase of the ($\Delta H_m - \Delta H_c$) value with the TLCP content is fairly noticeable. The relationship presented here further confirms the ability of TLCP to function as a nucleating agent, enhancing the formation of crystallites and the overall crystallization process of PEN.

The difference between the enthalpy of melting and that of the crystallization ($\Delta H_m - \Delta H_c$) plotted against different TUSs shows the change in crystallinity of the PEN matrix consequent to stretching the PEN/TLCP blends: the ($\Delta H_m - \Delta H_c$) value increases with increasing TUS (Fig. 8). The primary reason for this is presumably the orientation-induced crystallization of PEN. To discover the role TLCP plays in introducing this type of crystallization, we compared the data for the enthalpy change of three blending systems: pure PEN, PEN/30TLCP, and PEN/60TLCP. A linear re-

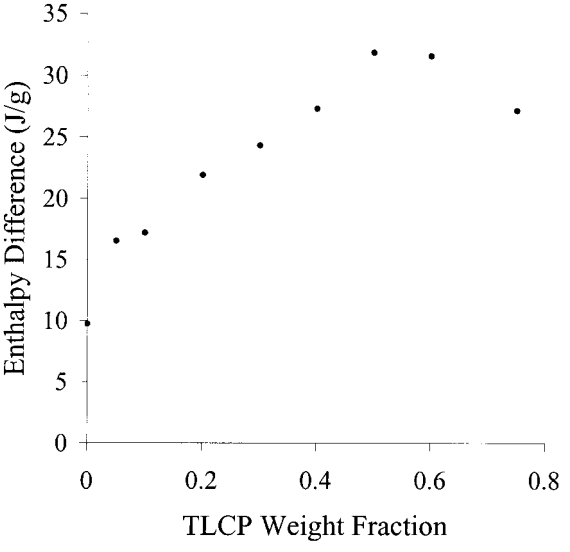

Figure 7 The variation of the crystallinity by the (•) enthalpy difference of PEN with a TLCP fraction at a take-up speed of 300 m/min.

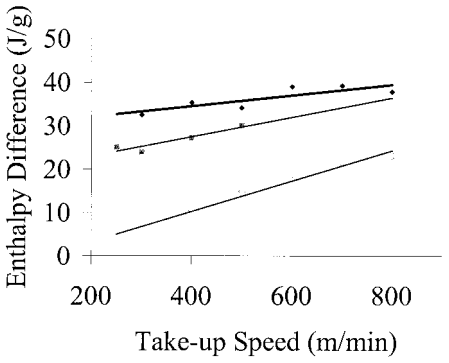

Figure 8 The enthalpy difference versus the winding speed for (◆) PEN/60TLCP, (■) PEN/30TLCP, and (○) PEN.

gression analysis of these data yields the following relationship for the three systems:

$$(\Delta H_m - \Delta H_c)_{\text{PEN/60TLCP}} = 0.0122V_L + 29.654 \quad (4)$$

$$(\Delta H_m - \Delta H_c)_{\text{PEN/30TLCP}} = 0.0223V_L + 18.577 \quad (5)$$

$$(\Delta H_m - \Delta H_c)_{\text{PEN}} = 0.035V_L - 3.7485 \quad (6)$$

where V_L represents the TUS. The observed difference in the slopes, that is, the rate of increase of the crystallinity with the TUS, indicates orientation-induced crystallization is restricted with the presence of the TLCP phase and that there is a coincident reduction in the orientation of PEN. A causal explanation is probably wind-up speed suppression (WUSS),[24] which was observed in other TLCP-containing systems. The WUSS is a consequence of shear being introduced into the elongational flow by the presence of minor phase fibrils, because the dispersed phase and the continuous phase are not deformed to the same extent. The result of this shear is a decrease of the molecular orientation of the matrix polymer along the fiber spinning direction. On the other hand, in the PEN/60TLCP blending system, in which we noted phase inversion, TLCP is the continuous phase while PEN exists as spherical inclusions. As the blend fiber is stretched, the actual force being exerted on the PEN phase is not the same as the force exerted on the fiber. Therefore, the extent of orientation of the PEN phase depends on how effectively the stress can be transferred from the TLCP major phase to the PEN minor phase, which in turn depends on the strength of the interface between the two phases. Generally, for an imperfectly miscible system this force is smaller than the actual force. If the preceding premises are accepted, the retardation of orientation-induced crystallization of PEN in the PEN/TLCP blends can be readily understood.

The melting temperatures of PEN/30TLCP and PEN/60TLCP blends decreased with increasing winding speed (Fig. 9). This phenomenon suggests the possibility of improving the miscibility of PEN/TLCP blends by increasing the TUS.

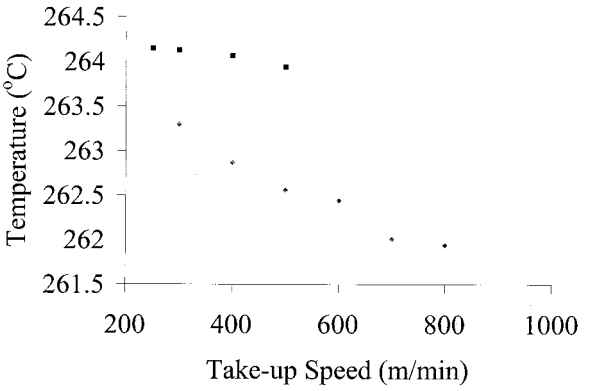

Figure 9 The variation of the melting temperature of PEN/TLCP blend fibers with the take-up speed for (◆) PEN/60TLCP and (■) PEN/30TLCP.

Raman spectroscopy

Raman spectroscopy is widely used to provide information on the average molecular orientation of both the amorphous and crystalline phases in a semicrystalline polymer.[25] However, there are only limited reports concerning its application in TLCP.[26] We used laser Raman spectroscopy in our study to provide

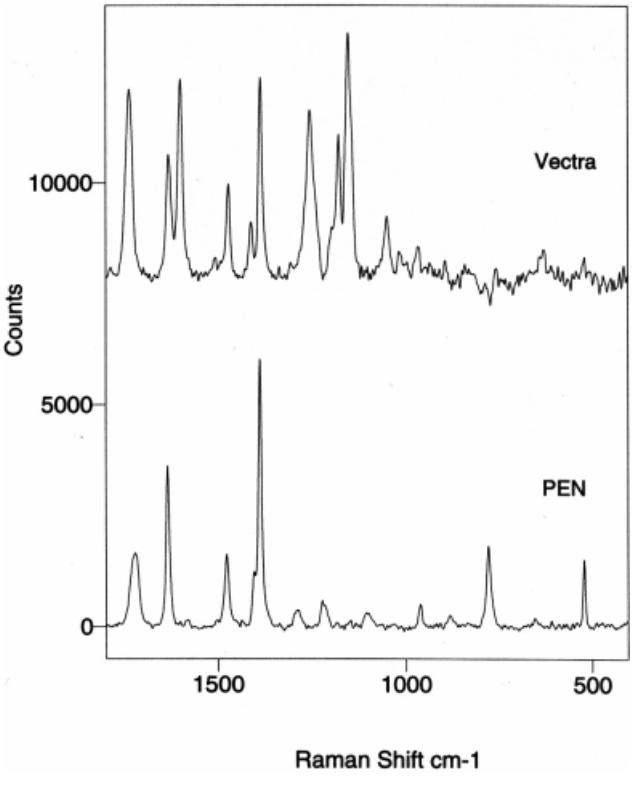

Figure 10 Unpolarized Raman spectra of PEN and Vectra A950.

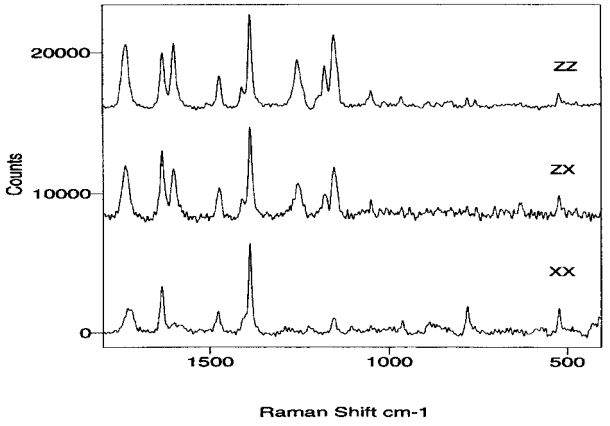

Figure 11 Raman spectra for the PEN/60TLCP fiber at a take-up speed of 300 m/min.

qualitative information about the orientation of TLCP in the PEN matrix in a manner based on our previous work.[3]

In order to determine the degree of molecular orientation, it is necessary to focus our attention on a specific peak in the spectrum. The Raman spectra of PEN and Vectra indicate that the 1599 cm^{-1} vibration band is unique to Vectra (Fig. 10). This band is associated with the C1–C4 stretching vibration of the benzene ring in Vectra.[27] As a result, this peak can be used to analyze the orientation of Vectra in the PEN matrix. In addition, there are two other reasons for choosing the 1599 cm^{-1} band. First, this ring stretch is not greatly perturbed upon substitution; therefore, this vibration is indicative of the presence of an aromatic ring. Second, this band is strong, fairly well resolved, and its intensity can be determined accurately.

Raman spectra utilizing selected polarization geometries (*ZZ*, *ZX*, *XX*) were obtained from the PEN/60TLCP blended fiber produced at various winding speeds. Comparing these spectra for winding speeds of 800 and 300 m/min (Figs. 11, 12), it is obvious that

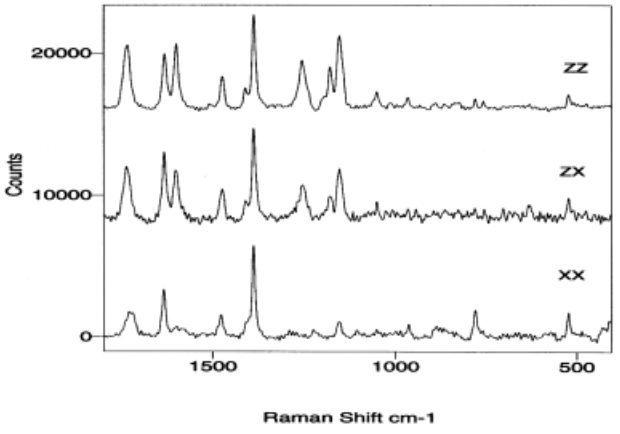

Figure 12 Raman spectra for the PEN/60TLCP fiber at a take-up speed of 800 m/min.

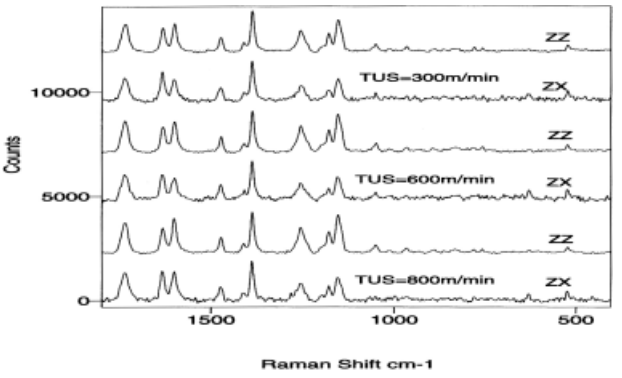

Figure 13 Raman spectra for the PEN/60TLCP blended fiber at selected take-up speeds.

the 1599 cm^{-1} vibration band is much more intense in the *ZZ* spectrum when compared to the spectra direction in the *ZX* or *XX* spectra. This indicates that the vibration is much stronger along the direction of drawing, implying a significant degree of molecular orientation along the stretching direction. There is a progressive change of the relative Raman intensities in the *ZZ* and *ZX* direction as the winding speed increases, showing the effect of the TUS on the orientability of Vectra in the PEN matrix (Fig. 13). Thus, in order to estimate the relative orientation in these fibers we selected the ratio $(I_{zz})_{1599}$ to $(I_{zx})_{1599}$, where I_{zz} and I_{zx} are the areas under the 1599 cm^{-1} vibration band in the *ZZ* and *ZX* direction, respectively. To account for the effect of the variable focus and incident laser power on the intensities of these bands, the 525 cm^{-1} band was used as an internal standard. This band is unique to PEN, and its intensity appears to be relatively unaffected by orientation in the sample.

The normalized Raman band intensities as a function of the TUS is plotted in Figure 14. Our data imply that the orientation of TLCP in the PEN matrix increases with the TUS. Further, over a limited range in the TUS in the neighborhood of 600 m/min, there is

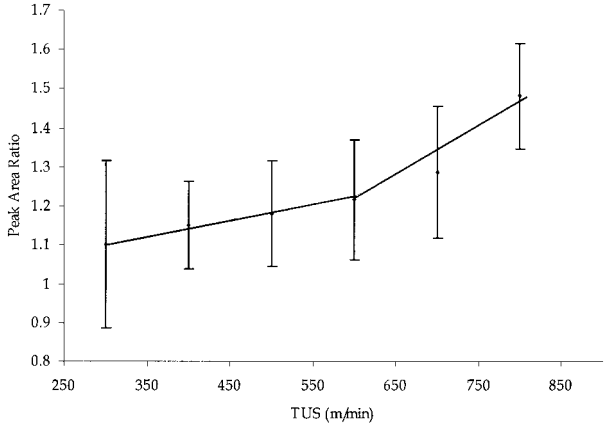

Figure 14 Raman estimation of the relationship between TLCP orientation and the take-up speed.

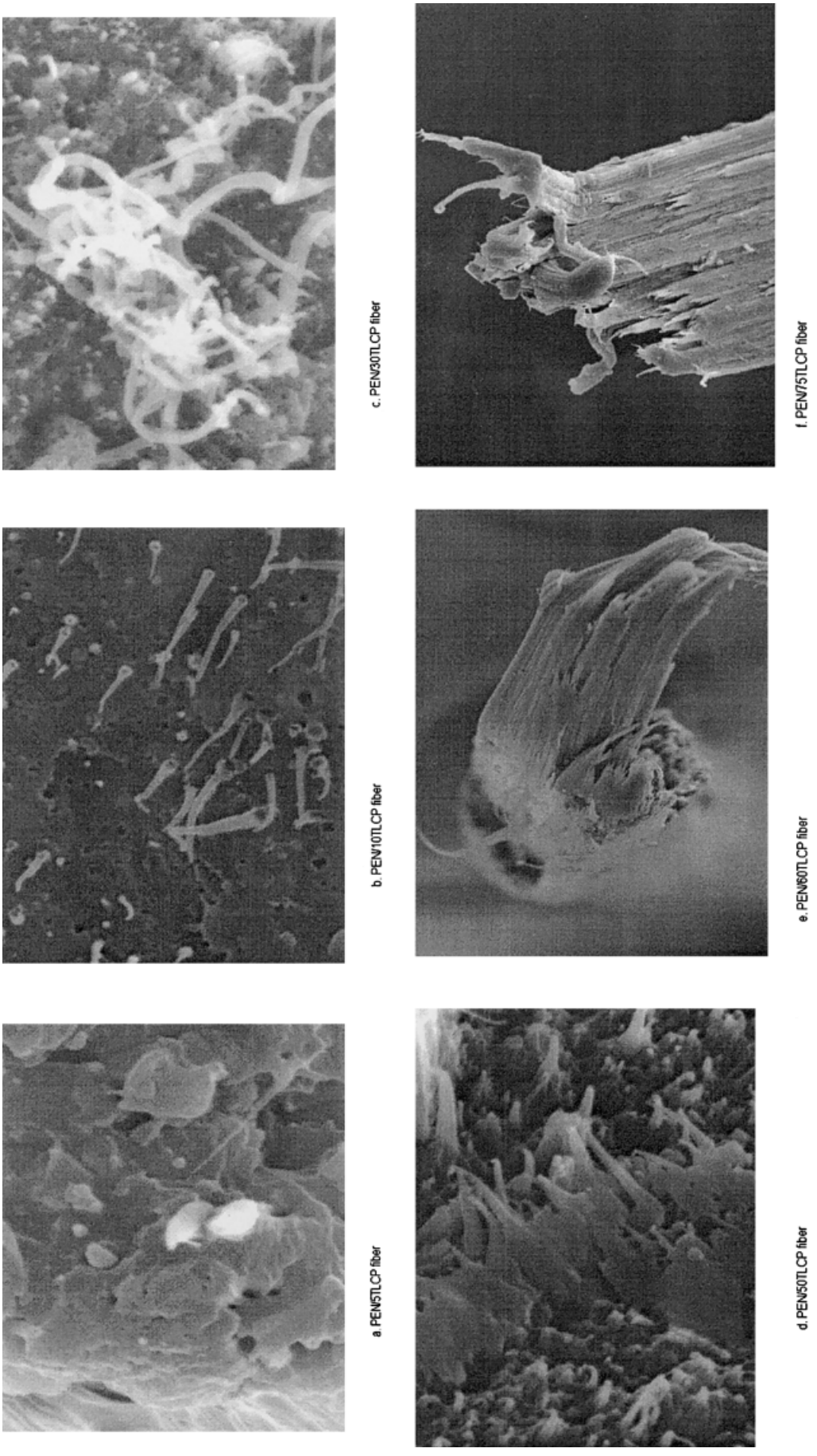

Figure 15 SEM photographs of PEN/TLCP blended fibers.

apparently a change in the rate of orientation development. To illustrate this we constructed two straight lines through the data as shown. A more detailed study on fibrillation of the minor phase and its dependency on composition using Raman spectroscopy is being carried out in our lab to further explore this hypothesis.

Morphology study

The SEM photomicrographs in Figure 3(a–f) illustrated the evolution of the TLCP morphology in the spinneret as the concentration of TLCP increases. The fracture surface presents a speckled appearance that is due to a large number of small TLCP domains scattered throughout the PEN matrix. At low concentration (<20 wt %) the TLCP appears to exist as smooth spheres anchored in the PEN matrix without any preferred orientation. Upon close examination, some open rings appear around the TLCP, presumably as a result of poor adhesion between the PEN and TLCP, which means much of the energy of stretching is dissipated in separating the TLCP from the PEN matrix rather than in deforming the TLCP into fibrils. At higher concentrations the TLCP domains are elongated and pulled out of the matrix during fracture, as evidenced by the smoothly tapering tips on some domains and the holes left in the matrix. Even so, the TLCP domains increase in number as the TLCP concentration increases and are highly aligned parallel to each other. At 60 wt % TLCP the phase inversion begins; the photomicrograph shows that TLCP forms the continuous phase. The variety of structures results from the complex interplay between the rheological properties of PEN and TLCP and the shearing and elongation flow inside the spinneret. Van Eijndhoven-Rivera et al.[28] reported the result of a study of the correlation among the rheology, morphology, and minor-phase orientation in TLCP-based polymer blends in simple shear and capillary flow using wide-angle X-ray diffraction methods. They found that the degree of molecular orientation depended on the amount of TLCP present in the blends and on the stress transfer condition between the two phases. The formation of continuous fibrils was accompanied by a high degree of orientation of the TLCP.

In the photomicrographs of Instron fractured blend fibers [Fig. 15(a–f)] one can see the effect of concentration on the morphology. For the 5 wt % blend, TLCP was sparsely dispersed as spheres on the fracture surface, implying no reinforcement between PEN and TLCP; for the 10 wt % blend, the TLCP achieved a small aspect ratio and protruded a little from the matrix. As the TLCP concentration approached 30 wt %, a significant morphology change took place: the morphology of the TLCP phase became one of highly elongated and highly parallel domains extending a considerable distance from the surface of the matrix. In addition, it can be seen that elongated sheetlike structures were being formed at a TLCP weight concentration over 50%. As a rule, it is generally accepted that the mechanical properties of *in situ* composites are greatly influenced by morphology.

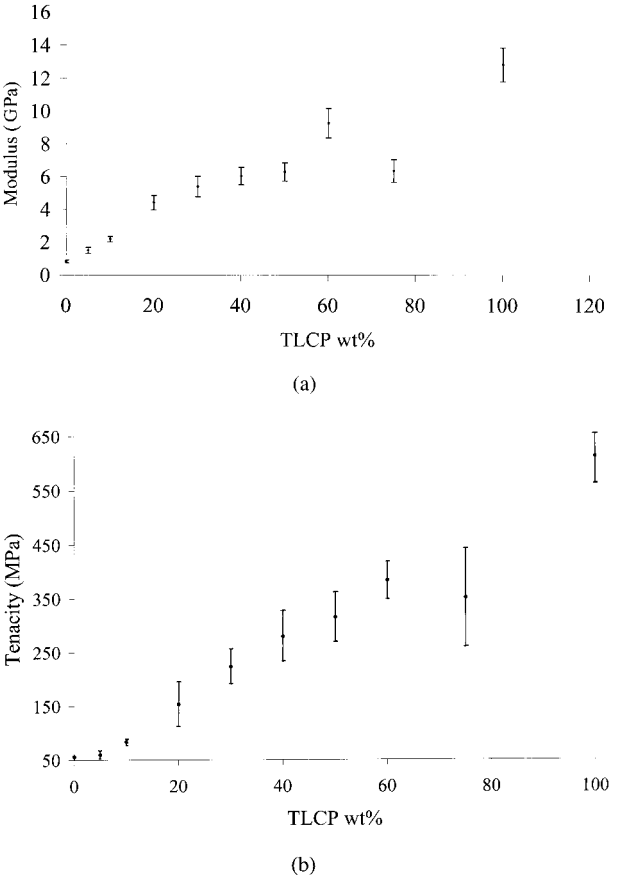

Figure 16 The relationship between the mechanical properties and TLCP concentration: (a) the modulus versus the TLCP content and (b) the tenacity versus the TLCP content.

Mechanical properties of pen/vectra a950 composite fibers

Our main purpose of utilizing TLCP as a blend component is to reinforce the matrix polymer by forming a fibrillar structure. In this final section we offer our present understanding of the mechanical properties of our PEN/TLCP composite fibers relative to their corresponding morphologies.

It is well accepted that blends of compatible polymers exhibit good mechanical properties; in particular, notice is taken of marked improvement in the tensile strength. Compatible systems exhibit tensile strength as a function of the blend composition that is a weighted average of the strength values of the two components. This phenomenon is a consequence of strong specific interaction that tends to lead to better

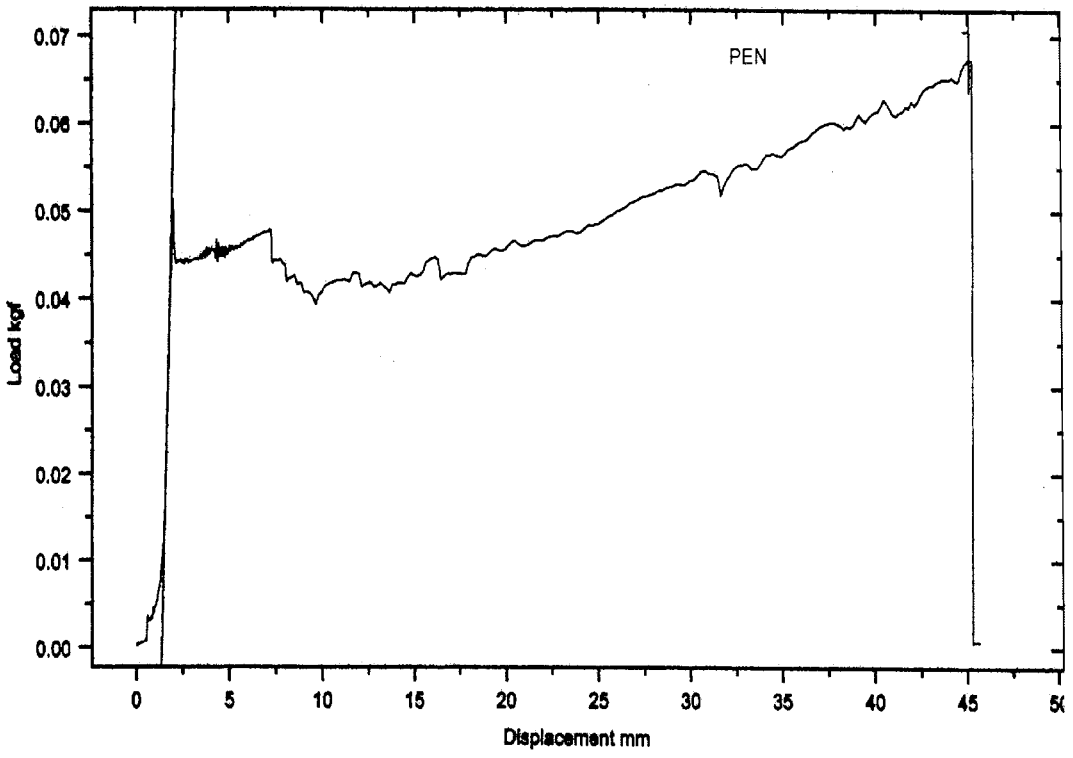

(a)

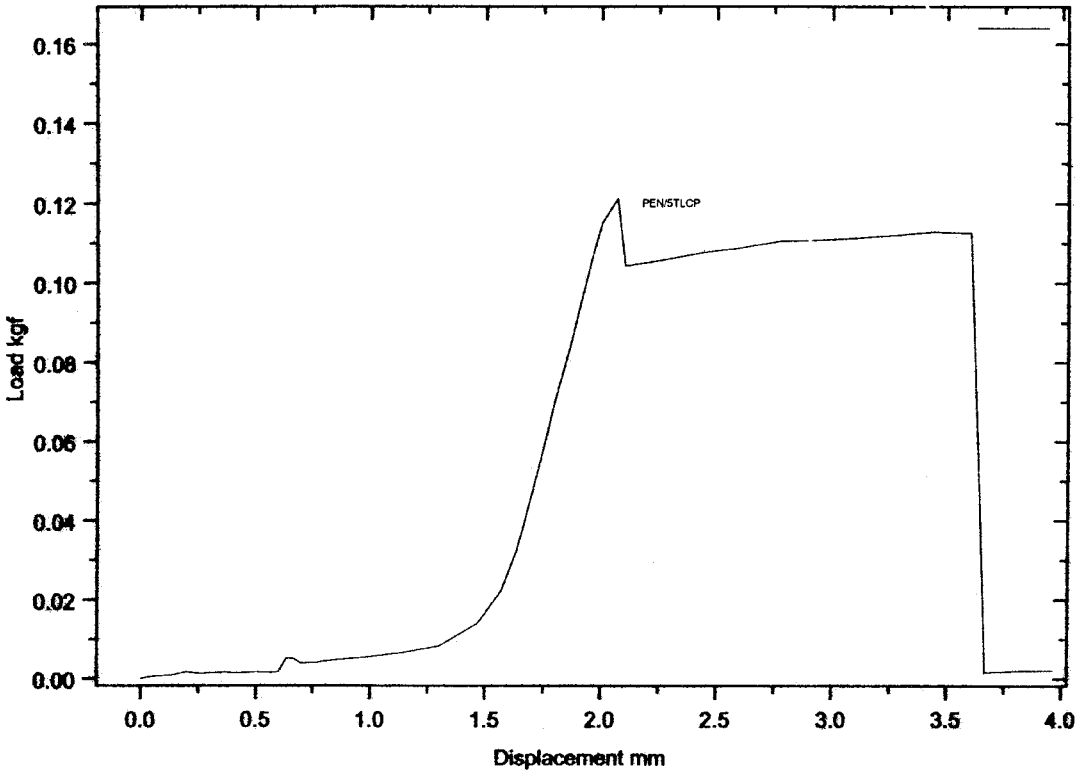

(b)

Figure 17 The stress–strain curve of PEN and PEN/5TLCP.

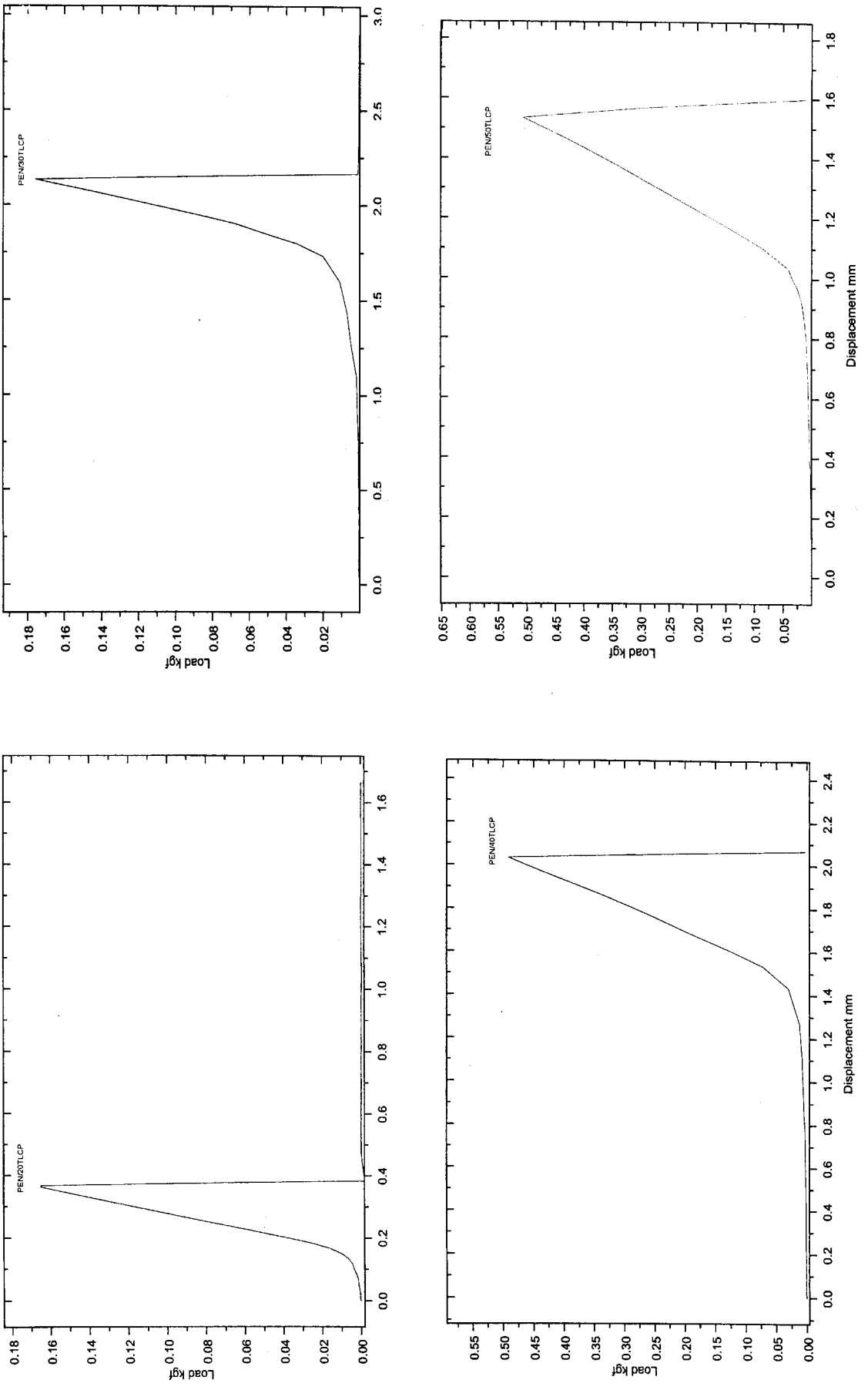

Figure 18 The stress–strain curves for PEN/TLCP blend fibers.

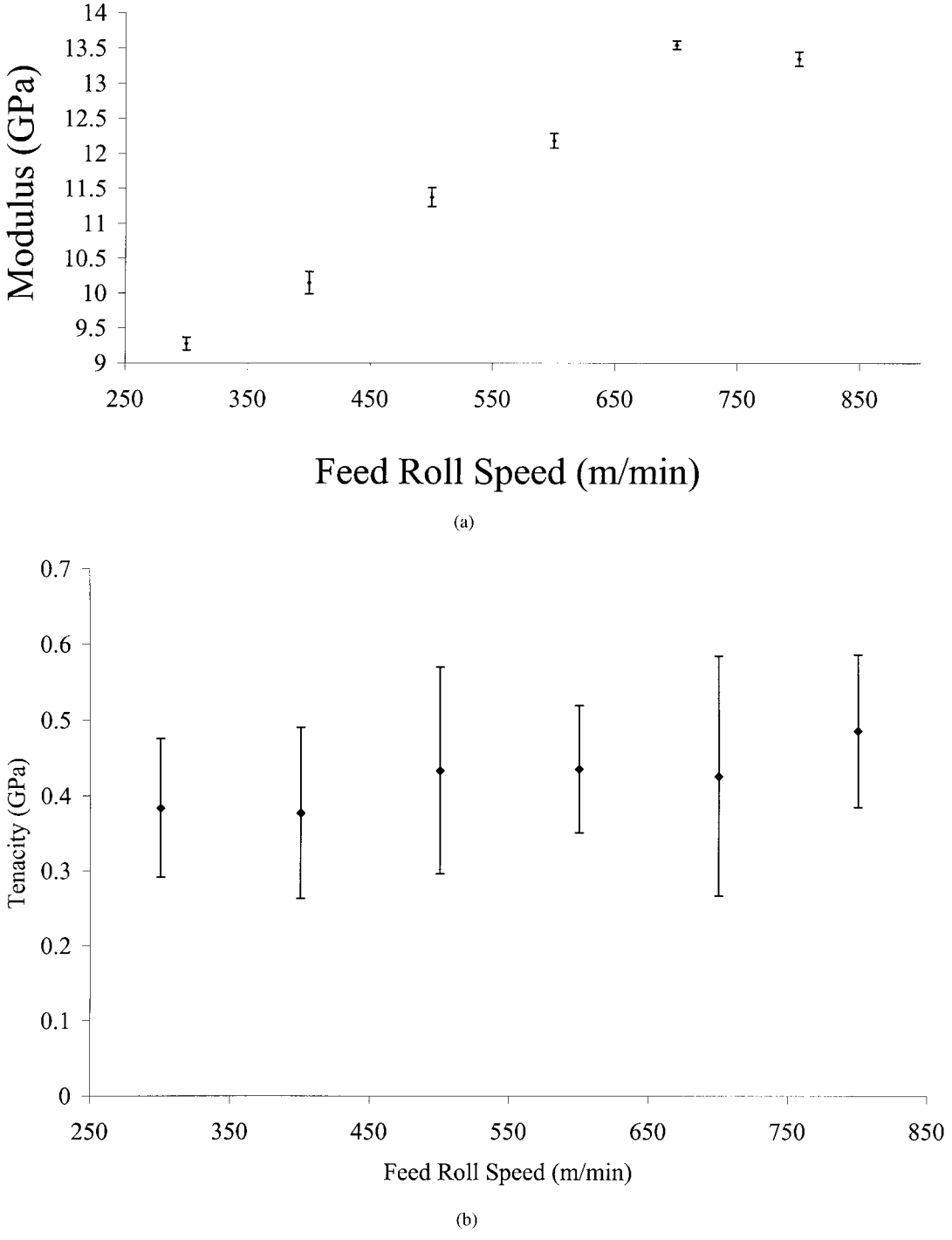

Figure 19 The relationship between the mechanical properties and winding speed. (a) the modulus versus the feed roll speed for PEN/60TLCP and (b) the Tenacity versus the feed roll speed for PEN/60TLCP.

molecular packing.[29] In contrast, blends of incompatible polymers reportedly exhibit a broad minimum in tensile strength as a function of composition.[30,31]

The tensile strength and modulus of all PEN/TLCP blend fibers are plotted versus the TLCP weight concentration in Figure 16(a,b). As expected, a fairly good linear relationship exists between the tenacity and TLCP concentration, suggesting a degree of miscibility between the PEN and TLCP phases. The 75 wt % blend deviates from this trend by exhibiting an abrupt drop-off in both the tensile strength and tensile modulus, presumably as a consequence of the phase separation we remarked upon earlier. The curve of the modulus versus the TLCP concentration can be divided into several regions with each region representing a particular TLCP morphology. The first region

covers the composition range from 0 to 10 wt % TLCP. The SEM photomicrographs [Fig. 15(a,b)] show a uniform dispersion of TLCP rigid spheres buried in the PEN matrix. There is no reinforcement between TLCP and PEN. In the second range of 20–50 wt % TLCP, TLCP exists as long fibrils with a rather large aspect ratio and most of those fibrils align themselves in the direction of flow [Fig. 15(c,d)]. The TLCP fibrils are formed in two steps. In the converging zone of the spinneret entrance the elongational flow deforms the dispersed TLCP spheres into fibrils. Because of the long relaxation time of TLCP, these fibrillar structures are preserved in the ensuing shear flow through the spinneret capillary. As soon as the TLCP fibrils emerge from the spinneret, they are further extended by the elongational flow field in the spin line. The reinforcing effect in this region is remarkable because the extensive formation of TLCP fibrils and their enhanced orientation necessitate a significant amount of stress transfer from the PEN matrix to the dispersed TLCP phase, which eliminates the possibility of slippage at the PEN–TLCP interface. This mechanism was evidenced by van Eijndhoven-Rivera et al. during their study of the morphology of a PBT/TLCP blend.[28] From 50 to 60 wt % TLCP there is a significant increase in modulus of the blend fibers. The previous SEM photomicrographs suggest that phase inversion occurs at 60 wt % TLCP; the TLCP now being the major phase, the mechanical properties of the blend fibers are dominated by the TLCP phase. Finally, at the phase separation point the modulus shows an obvious drop, as shown by the DSC results.

The stress–strain behavior in these three regions also shows some changes corresponding to changes in the composition. In the first region the stress–strain curve is generally similar to that of PEN (Fig. 17). There is a yield point, followed by elongation at almost constant stress; finally, the fibers exhibit strain hardening and then break. However, the strain at the breaking point is significantly decreased from 381% for neat PEN to 4% at 5 wt % TLCP (Fig. 17). On the other hand, the composite fibers have a higher modulus compared to pure PEN. In regions II and III, where the composite fibers contain a large amount of TLCP, the stress–strain behavior is totally different. No yield point on the stress–strain curve or necking appears on the fibers: the curve swings upward rather sharply near the end of the deformation (Fig. 18).

The modulus [Fig. 19(a)] of the blend fibers increases significantly with the TUS; however, the effect on the tenacity is not so remarkable [Fig. 19(b)]. A much higher TUS than our equipment can presently attain would appear to be required to achieve a significant increase in tenacity. The TLCP gives rise to a highly organized liquid phase upon melting, the domains of which tend to spontaneously pack parallel to one another and form highly ordered domains. Under elongational processing conditions these oriented domains develop a fibrilar morphology with a high aspect ratio (L/D). The correlation of our Raman data (Fig. 14) with the measured mechanical properties [Fig. 19(a,b)] suggests the two-step development of the TLCP microstructure within the PEN matrix. At a TUS below 600 m/min there is not much difference in the TLCP orientation in the blend fibers collected at selected wind-up speeds; accordingly, the tenacity of the fiber within this TUS region remains approximately constant. However, the modulus shows a continuous increase with the increase of the TUS. We believe this increase is probably attributable to the continuous deformation of TLCP droplets to high aspect ratio TLCP fibrils, while the orientation of these fibrils within the fiber is not fully developed. The dependency of the fiber modulus on the aspect ratio of the TLCP fibrils was quantitatively described in the Tsai–Halpin equation.[32] At a TUS above 600 m/min the modulus of the fiber levels off while the tenacity value shows a slight increase. The Raman data in this TUS region shows an accelerating development of TLCP orientation. In summary, TLCP fibril orientation begins to evolve when TLCP droplets are deformed to a certain extent. In order to obtain fibers with both high modulus and tenacity, the existence of highly oriented TLCP fibrils is necessary. Attaining this morphology requires use of a high TUS.

CONCLUSION

A series of fibers based on PEN and Vectra A950 was prepared. Fibrillation of Vectra A950 began when its concentration in the blend was over 10 wt %. The effects of the Vectra A950 content and winding speed on the morphology and properties of composite fibers were examined. We found that the PEN/Vectra A950 blending system was partly miscible and that the Flory–Huggins interaction parameter determined by the Nashi–Wang equation was -0.146. Two primary effects resulting from adding Vectra A950 into PEN were observed: Vectra A950 acted as a nucleating agent to enhance the crystallization process of PEN during melt spinning, and the reinforcing effect was evidenced by an enhancement in the mechanical properties. A fairly good linear relationship was found between the tenacity and weight concentration of Vectra A950. Increasing the TUS improved the mechanical properties of PEN/TLCP blend fibers and the miscibility of the blending system.

The net degree of molecular orientation of TLCP in the blend was evaluated from laser Raman spectroscopy. The peak area ratio representing the molecular alignment could be determined using the ZZ and ZX spectrum of the 1599 cm^{-1} vibration band, which was related to the benzene ring stretching. The results

show that a high TUS is necessary to orient the Vectra A950 phase.

The authors would like to thank the National Science Foundation for funding.

References

1. Dutta, D.; Fruitwala, H.; Kohli, A.; Weiss, R. A. Polym Eng Sci 1990, 30, 1005.
2. La Mantia, F. P.; Roggero, A.; Pedretti, U.; Magagnini, P. L. In Liquid-Crystalline Polymer Systems: Technological Advances; Iasyev, A. I., Ed.; American Chemical Society: Washington, DC, 1996.
3. Paradkar, R. P.; Sakhalkar, S. S.; He, X.; Ellison, M. S. Appl Spectrosc 2001, 55, 534.
4. Porto, S. P. J. J Opt Soc Am 1966, 56, 1585.
5. Paul, D. R. In Polymer Blends; Paul, D. R., Newman, S., Eds.; Academic: New York, 1978; Chapter 16.
6. Baird, D. G.; Sun, T. In Liquid-Crystalline Polymer; Weiss, R. A., Ober, C. K., Eds.; American Chemical Society: Washington, DC, 1990.
7. Juha, Sa.; Tokmala, P. J Appl Polym Sci 1989, 40, 453.
8. Haile, A. W.; Caldwell, J. K. Eastman Chemical Company document, personal communication.
9. Lin, Y. G.; Winter, H. H. Macromolecules 1988, 21, 2439.
10. Jun, X.; Tai, S. J Appl Polym Sci 1999, 73, 2195.
11. Blizard, K. G.; Baird, D. G. Polym Eng Sci 1987, 27, 653.
12. Weiss, R. A.; Huh, W.; Nicolais, L. Polym Eng Sci 1987, 27, 684.
13. Blizard, K. G.; Federici, C.a; Federico, O.; Chapoy, L. L. Polym Eng Sci 1990, 30, 1442.
14. Lewin, M.; Preston, J. Handbook of Fiber Science and Technology, Volume III: High Technology Fibers; Marcel Dekker: New York, 1983; Part A.
15. Tovar, G.; Carreau, P. J.; Schreiber, H. P. Colloids Surfaces A Physicochem Eng Aspects 2000, 161, 213.
16. Tang, P.; Jeffrey, A.; Reimer, M.; Denn, M. Macromolecules 1996, 26, 4269.
17. Nishi, T.; Wang, T. T. Macromolecules 195, 8, 909.
18. Scott, R. L. J Chem Phys 1949, 17, 279.
19. Bucher, S.; Wiswe, D.; Zachamm, H. G. Polymer 1989, 30, 480.
20. Van Krevelen, D. W. Properties of Polymers: Their Correlation with Chemical Structure; Their Numerical Estimation and Prediction from Additive Group Contributions; Elsevier: New York, 1990; Chapter 19.
21. Herlingen, H.; Hirt, P.; Koch, W.; Schautler, H. P. Lenzinger Ber 1977, 43, 24.
22. Kim, W. N.; Morton, M.; Denn, M. J Rheol 1992, 36, 1447.
23. Paci, M.; Liu, M.; Magagnini, P. L.; La Mantia, F. P.; Valenza, A. Thermochimica 1988, 137, 105.
24. Brody, H. J Appl Polym Sci 1988, 31, 2753.
25. Everall, N.; Chalmers, J.; Thomas, J. W. Polymer 1988, 29, 437.
26. Voyiatzis, G.; Petekidis, G.; Vlassopoulos, D.; Kamitsos, I. E.; Bruggeman, A. Macromolecules 1996, 29, 2244.
27. Dollish, R. F.; Fateley, W. G.; Bentley, F. F. Characteristic Raman Frequencies of Organic Compounds; Wiley–Interscience: New York, 1973; Chapter 13.
28. van Eijndhoven-Rivera, M. J.; Wagner, N. J.; Hsiao, B. J Polym Sci Part B Polym Phys 1998, 36, 1769.
29. MacKnight, W. J.; Karaasz, F. E.; Fried, J. R. Polymer Blends; Paul, D. R., Newman, S., Eds.; Academic: New York, 1978; Chapter 5.
30. Perry, E. J Appl Polym Sci 1964, 8, 2605.
31. Feldman, D.; Rusu, M. Eur Polym J 1974, 10, 41.
32. Halpin, J. C.; Kardos, J. L. Polym Eng Sci 1976, 16, 344.